REGULAR ARTICLE

blood advances

IL-6–driven POU2AF1 and ELL2 are key regulators of multiple myeloma–distinct transcriptional and splicing programs

Yasuyo Ohguchi,[1,*] Masahiko Ajiro,[2,*] Daisuke Ogiya,[3] Takeshi Masuda,[4] Yawara Kawano,[5] Shingo Usuki,[6] Tomoaki Koga,[7] Shinjiro Hino,[7] Takeshi Harada,[8] Satoru Takahashi,[9] Seiji Okada,[10] Jun-ichirou Yasunaga,[5] Goro Sashida,[11] Sumio Ohtsuki,[12] Mitsuyoshi Nakao,[7] Takashi Minami,[13] Akihide Yoshimi,[2] and Hiroto Ohguchi[1]

[1]Division of Disease Epigenetics, Institute of Resource Development and Analysis, Kumamoto University, Kumamoto, Japan; [2]Division of Cancer RNA Research, National Cancer Center Research Institute, Tokyo, Japan; [3]Department of Hematology and Oncology, Tokai University School of Medicine, Isehara, Japan; [4]Institute for Advanced Biosciences, Keio University, Tsuruoka, Japan; [5]Department of Hematology, Rheumatology, and Infectious Diseases, Graduate School of Medical Sciences, Kumamoto University, Kumamoto, Japan; [6]Liaison Laboratory Research Promotion Center and [7]Department of Medical Cell Biology, Institute of Molecular Embryology and Genetics, Kumamoto University, Kumamoto, Japan; [8]Department of Hematology, Endocrinology and Metabolism, Tokushima University Graduate School of Biomedical Sciences, Tokushima, Japan; [9]Department of Anatomy and Embryology, Institute of Medicine, University of Tsukuba, Tsukuba, Japan; and [10]Division of Hematopoiesis, Joint Research Center for Human Retrovirus Infection, [11]Laboratory of Transcriptional Regulation in Leukemogenesis, International Research Center for Medical Sciences, [12]Department of Pharmaceutical Microbiology, Faculty of Life Sciences, and [13]Division of Molecular and Vascular Biology, Institute of Resource Development and Analysis, Kumamoto University, Kumamoto, Japan

Key Points

- IL-6–driven POU2AF1 and ELL2 confer the robustness of MM-distinct transcriptional program.
- POU2AF1 is also engaged in the organization of nuclear speckles and IL6–mediated alternative RNA splicing.

Multiple myeloma (MM) is a plasma cell neoplasm that depends on the bone marrow (BM) microenvironment; however, the underlying mechanisms of epigenetic contribution to the pathogenesis of MM are incompletely understood. Here, we delineate epigenetically driven transcriptional and splicing regulation crucial for MM. We recharacterized the transcriptional program induced by interleukin 6 (IL-6)/Janus kinase (JAK)/signal transducer and activator of transcription 3 (STAT3) pathway by integrating chromatin immunoprecipitation sequencing, transcriptomic analyses, and CRISPR knockout screening, identifying the B-cell lineage factors POU2AF1 and ELL2, as crucial IL-6/JAK/STAT3 targets essential for MM cell growth and survival. Genetic depletion of these factors significantly suppressed MM cell growth in vitro and in the xenograft model of IL-6 humanized mice. Mechanistically, POU2AF1 and ELL2 form an autoregulatory loop with IRF4 and establish an MM-distinct transcriptional program representing cellular immaturity. The IL-6/JAK/STAT3 pathway augments this program by upregulating and recruiting these factors to MM signature genes. Furthermore, POU2AF1 and ELL2 are essential in the regulation of IL-6–dependent alternative RNA splicing. Immunocytochemical and proteomic analyses revealed that POU2AF1 colocalizes and facilitates formation of nuclear speckles, where it interacts with trans-acting splicing factors required for MM cell growth. These findings suggest dual roles of POU2AF1 and ELL2 in coordinating transcription and RNA splicing to generate MM-associated mRNA isoforms. Finally, we showed that gapmer antisense oligonucleotides targeting POU2AF1 reduced MM cell growth in the presence of soluble BM stromal cell factors, including IL-6.

Submitted 10 October 2025; accepted 15 February 2026; prepublished online on *Blood Advances* First Edition 2 April 2026. https://doi.org/10.1182/bloodadvances.2025018710.

*Y.O. and M.A. contributed equally to this study.

Chromatin immunoprecipitation sequencing and RNA sequencing data have been deposited at the Gene Expression Omnibus database (accession numbers GSE298692, GSE298693, and GSE298694). Proteomics mass spectrometry raw data have been deposited at the Japan Proteome Standard Repository database (accession number JPST003804).

The full-text version of this article contains a data supplement.

Our data demonstrate that IL-6–driven B-cell lineage factors are the vulnerability of MM cells and may represent novel therapeutic targets for this incurable tumor.

Introduction

Multiple myeloma (MM) is an incurable plasma cell neoplasm that depends on the bone marrow (BM) for its progression.[1] A key factor in the MM BM microenvironment is interleukin-6 (IL-6), which was first identified as a B-cell differentiation factor,[2] and soon recognized as a critical factor for MM cell growth.[3,4] IL-6 transgenic mice develop spontaneous plasmacytoma,[5,6] and primary human MM cells can be engrafted in the BM of humanized mice that express the human *IL-6* gene.[7] Furthermore, BM stromal cells (BMSCs) from patients with MM produce high amounts of IL-6.[8,9] Importantly, the *IL-6R* gene, located on chromosome 1q21, is frequently amplified in MM cells.[10] IL-6 activates several signaling pathways through its receptor complex, including Janus kinase (JAK)/signal transducer and activator of transcription (STAT), mitogen-activated protein kinase, and phosphatidylinositol-3 kinase/AKT signaling pathways,[11] with the JAK/STAT3 pathway being essential for MM cell growth and survival.[12] STAT3 upregulates antiapoptotic genes such as *MCL1*, although its full role extends beyond this upregulation.[12]

POU2AF1 (also known as BOB1/OBF1/OCAB) is a lymphoid cell-specific transcriptional coactivator that interacts with POU transcription factors POU2F1 (OCT1) and POU2F2 (OCT2) at octamer motifs (5′-ATGCAAAT-3′), thereby facilitating octamer-dependent transcription.[13-15] It is expressed throughout B-cell development,[16] with increased levels in germinal center (GC) B cells.[17,18] POU2AF1-deficient mice lack GC formation after immunization, resulting in reduced secondary immunoglobulin (Ig) isotypes and skewed Ig repertoires.[19-22] A recent genome-wide study revealed that POU2AF1 regulates genes involved in GC formation and is crucial for GC-derived lymphomas.[23-26] POU2AF1 is also highly expressed in MM, which is nevertheless a post GC-derived tumor.[27-29] Copy number alternation represents 1 potential mechanism underlying elevated expression, although amplification of the POU2AF1 region is relatively infrequent in MM.[27] Importantly, recent research identifies POU2AF1 as an essential factor for MM survival through the IRF4 network.[30] However, the mechanism of POU2AF1 induction beyond gene amplifications, as well as its precise molecular functions in MM, has not been fully deciphered.

ELL2, a member of the ELL family and part of the super elongation complex, promotes transcription elongation by releasing RNA polymerase II from transcriptional pausing.[31-33] In B cells, ELL2 is involved in the maturation of plasma cells and promotes Ig secretion by shifting Ig heavy chain mRNA from the membrane-bound to the secretory form alongside other super elongation complex components.[34,35] It also regulates gene expression and RNA splicing related to plasma cell differentiation, including unfolded protein response genes.[36-38] B-cell–specific *Ell2* knockout (KO) mice exhibit reduced numbers of plasma cells and decreased Ig secretion.[37] Recent genome-wide association studies have identified several MM risk variants at the *ELL2* locus that are associated with lower ELL2 expression.[39-43] Nevertheless, ELL2 expression is higher in MM than that in other types of cancers.[44]

Here, we recharacterize the IL-6/JAK/STAT3–driven transcriptional program in MM and identify *POU2AF1* and *ELL2* as key STAT3 targets essential for MM cell survival. POU2AF1 and ELL2 direct a unique MM transcriptional profile induced by IL-6. POU2AF1 is also associated with splicing factors essential for MM cells and involved in IL-6–mediated splicing regulation. These findings provide novel insights into the integrated transcriptional and splicing programs shaped by the BM environment in MM, and redefine the biological significance of IL-6 in MM.

Materials and methods

Primary patient samples and animal studies

BM samples were obtained from patients with MM after receiving informed consent and approval by the institutional review board of Kumamoto University.

Statistical analysis

Two-tailed Student *t* test was performed to determine significance between 2 groups. Log-rank test was conducted to determine the significance of survival differences using GraphPad Prism 9 software. A value of $P < .05$ was considered statistically significant.

Additional methods are described in detail in the supplemental Methods.

Animal studies were performed under a protocol approved by the Kumamoto University Animal Care and Use Committee. This study was conducted in accordance with the Declaration of Helsinki.

Results

Identification of crucial IL-6/JAK/STAT3 targets in MM

Although the IL-6/JAK/STAT3 pathway is crucial for MM cells, its epigenetic and transcriptional effects on MM cells have not been fully characterized. Therefore, we first examined the effect of IL-6 on histone modifications using the IL-6–responsive MM cell line, MM.1S. Chromatin immunoprecipitation followed by sequencing (ChIP-seq), normalized to reference exogenous genome, demonstrated that H3K4me3 and H3K27ac signals around transcriptional start sites were increased 4 hours after IL-6 treatment, whereas H3K27me3 signal was modestly decreased at the same time point (Figure 1A), suggesting that IL-6 promotes global transcriptional activation through epigenetic modification. We next sought to identify novel IL-6/JAK/STAT3 targets in MM cells. We performed ChIP-seq for phosphorylated STAT3 at tyrosine 705 (p-STAT3) after IL-6 treatment. Motif analysis of p-STAT3 ChIP-seq identified STAT3 motif as the most significantly enriched (Figure 1B), and we observed p-STAT3 binding at the *SOCS3* locus, a canonical STAT3 target gene (supplemental Figure 1A),

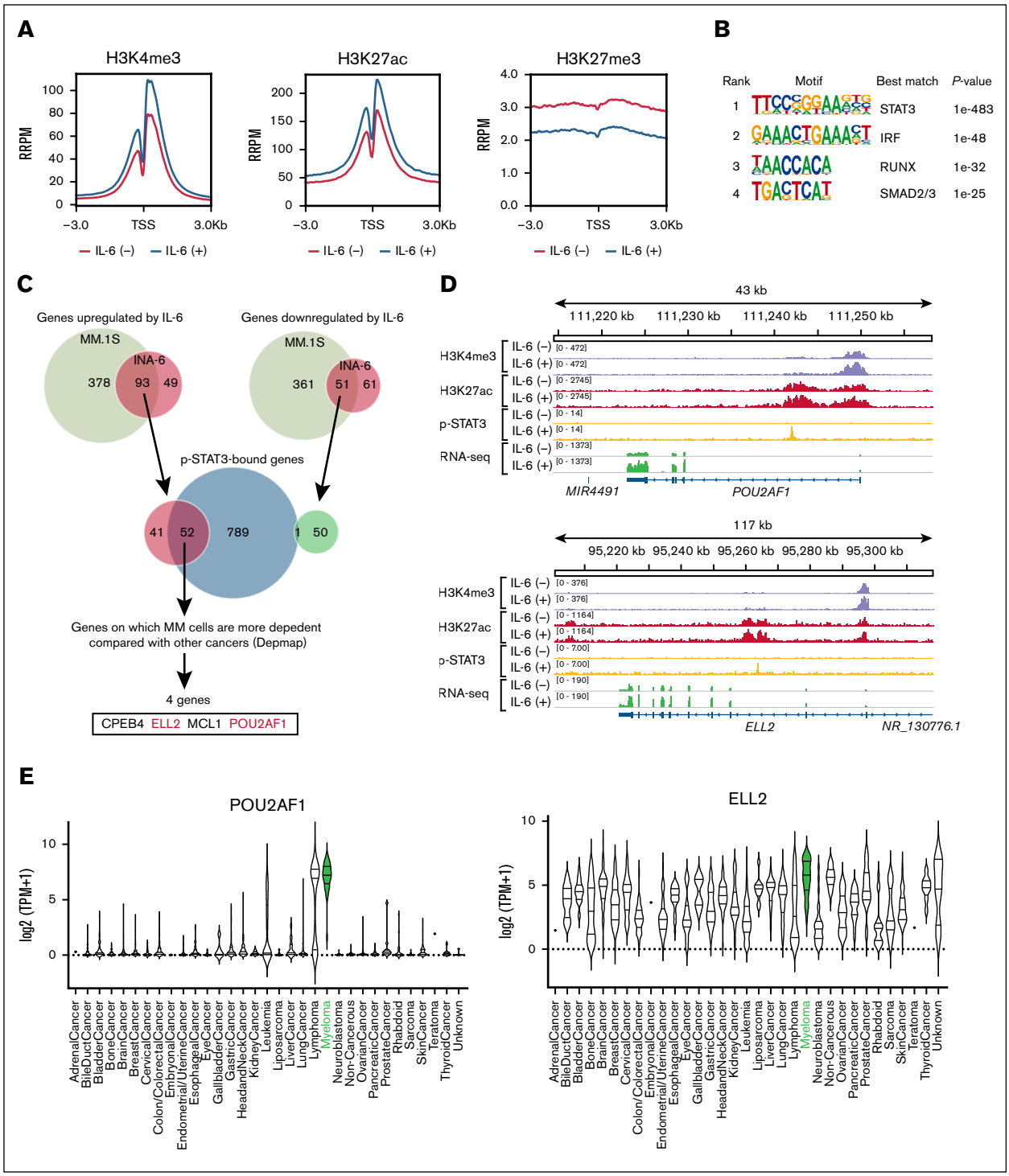

Figure 1. Identification of crucial IL-6/JAK/STAT3 targets in MM. (A) ChIP-seq signals of H3K4me3, H3K27Ac, and H3K27me3 at transcription start sites after treatment with or without IL-6 (10 ng/mL) for 4 hours in MM.1S cells. ChIP-seq signals were normalized to reference exogenous spiked-in *Drosophila* chromatin. (B) Motif analysis of ChIP-seq for phosphorylated (p)-STAT3 at tyrosine 705 after treatment with IL-6 (10 ng/mL) for 4 hours in MM.1S cells. The top 4 enriched motifs are shown. (C) Scheme for identifying crucial IL-6/JAK/STAT3 targets in MM. (D) Integrative Genomics Viewer tracks showing H3K4me3, H3K27Ac, p-STAT3, and mRNA signals at the *POU2AF1* and *ELL2* gene loci after treatment with or without IL-6 (10 ng/mL) for 4 hours in MM.1S cells. (E) Violin plots representing expression levels of *POU2AF1* and *ELL2* in a series of cancer cell lines. (F) Violin plots representing relative dependence of MM cell lines on POU2AF1 and ELL2 compared with other types of cancer cell lines. Panels E-F: data were downloaded from DepMap portal (https://depmap.org/portal/). Center lines represent the median, and lower and upper lines represent the interquartile range. RRPM, reference-normalized reads per million.

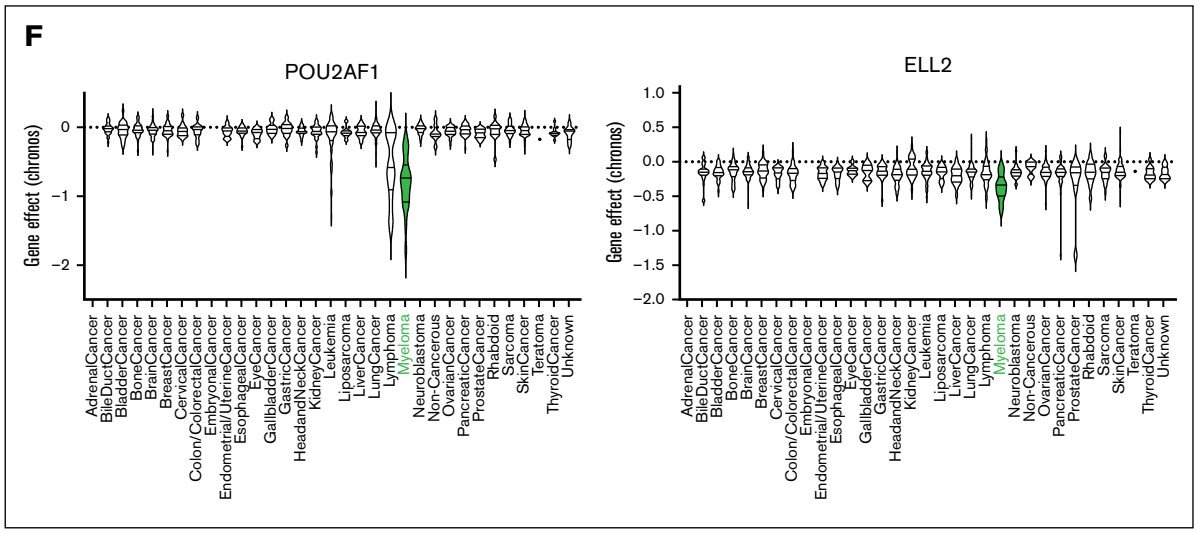

Figure 1 (continued)

validating the specificity of the p-STAT3 ChIP-seq. We then performed RNA sequencing (RNA-seq) analysis and combined this with p-STAT3 ChIP-seq results. Through RNA-seq analysis, we found that a total of 93 genes were upregulated, whereas 51 genes were downregulated (fold change $>2^{0.5}$ and adjusted $P <$ .05) after 4 hours of IL-6 treatment in both IL-6–responsive and IL-6–dependent MM cell lines (MM.1S and INA-6) (Figure 1C; supplemental Tables 1-3). Among 93 upregulated genes, 52 genes were bound by p-STAT3, whereas among 51 downregulated genes, only 1 gene was bound by p-STAT3, indicating that IL-6/JAK/STAT3 signaling predominantly activates target gene transcription in the context of MM cells, which was consistent with histone modification profiles (Figure 1C; supplemental Tables 4 and 5). We further analyzed the 52 IL-6–upregulated and p-STAT3–bound genes using DepMap, a comprehensive clustered regularly interspaced short palindromic repeat (CRISPR) KO screening database of a series of cancer cell lines (https://depmap.org/portal/).[45] Importantly, MM cells were more dependent on 4 genes than other cancers (effect size, less than -0.2 and $P < 10^{-7}$; myeloma cell lines vs others) (Figure 1C; supplemental Table 6). This gene list included a known STAT3 target in MM, *MCL1*, a member of the B-cell lymphoma 2 family exerting anti-apoptotic effect (supplemental Figure 1B-D).[12] Among these 4 genes, we focused on 2 genes, *POU2AF1* and *ELL2*, that are B-cell lineage–associated transcriptional cofactors (Figure 1D). POU2AF1 was exclusively expressed in MM and B-cell lymphoma cell lines among a series of cancer cell lines (Figure 1E). Although ELL2 was expressed in most of the cancer cell lines, it exhibited higher expression levels in MM cell lines relative to others (Figure 1E). Consistent with their expression levels, CRISPR KO screening data showed higher dependence of MM cell lines on POU2AF1 and ELL2 compared with other cancer cell lines (Figure 1F).

We next confirmed that the IL-6/JAK/STAT3 pathway mediates the induction of POU2AF1 and ELL2 in MM cells. STAT3 phosphorylation was observed 30 minutes after IL-6 treatment and remained elevated. Accordingly, POU2AF1 and ELL2 mRNA levels began to increase 2 hours after IL-6 stimulation, peaked at 4 hours, and were followed by increased protein expression (Figure 2A-B; supplemental Figure 2A-B). IL-6 at a concentration of 1 ng/mL sufficiently induced POU2AF1 and ELL2 expression (Figure 2A-B). We therefore used IL-6 at this concentration for experiments thereafter. We further validated IL-6–mediated POU2AF1 and ELL2 induction in additional MM cell lines (NCI-H929, KMS-12-BM, KMS-28-BM, and RPMI8226) and multiple primary cells from patients with MM (Figure 2C; supplemental Figure 2C-D). To test the requirement of STAT3 in the POU2AF1 and ELL2 induction, we transduced MM.1S cells stably expressing Cas9 with single-guide (sg) RNAs targeting *STAT3* (sgSTAT3 #1 and #2) or a control sgRNA targeting enhanced green fluorescent protein (*EGFP*) (sgEGFP) by lentivirus. KO of STAT3 largely abrogated IL-6–mediated POU2AF1 and ELL2 induction in MM.1S cells (Figure 2D-E). Together, these results demonstrated that POU2AF1 and ELL2 are direct targets of the IL-6/JAK/STAT3 pathway in MM cells.

POU2AF1 and ELL2 promote MM cell growth and survival in the BM environment

We next investigated the effect of KO of *POU2AF1* and *ELL2* on MM cell growth in the BM environment. We introduced sgRNAs targeting *POU2AF1* (sgPOU2AF1 #1 and #2), *ELL2* (sgELL2 #1 and #2), or *EGFP* (sgEGFP) into MM cell lines expressing Cas9, and validated depletion of each of the proteins (Figure 3A-B; supplemental Figures 3A-B and 4A-D). Consistent with the DepMap database and recent CRISPR studies,[45,46] KO of *POU2AF1* and *ELL2* inhibited the growth of 3 MM cell lines (MM.1S, INA-6, and MOLP-8) in the absence of IL-6 (Figure 3A-B). Importantly, IL-6 stimulated the growth of these MM cell lines, and this effect was largely abolished by KO of *POU2AF1* and *ELL2* (Figure 3A-B). Conditioned medium from BMSCs derived from patients with MM also increased POU2AF1 and ELL2 expression and stimulated MM cell growth. KO of *POU2AF1* and *ELL2* mostly abrogated this growth induction (supplemental Figure 3A-B). These results suggest that POU2AF1 and ELL2 contribute to MM cell growth within

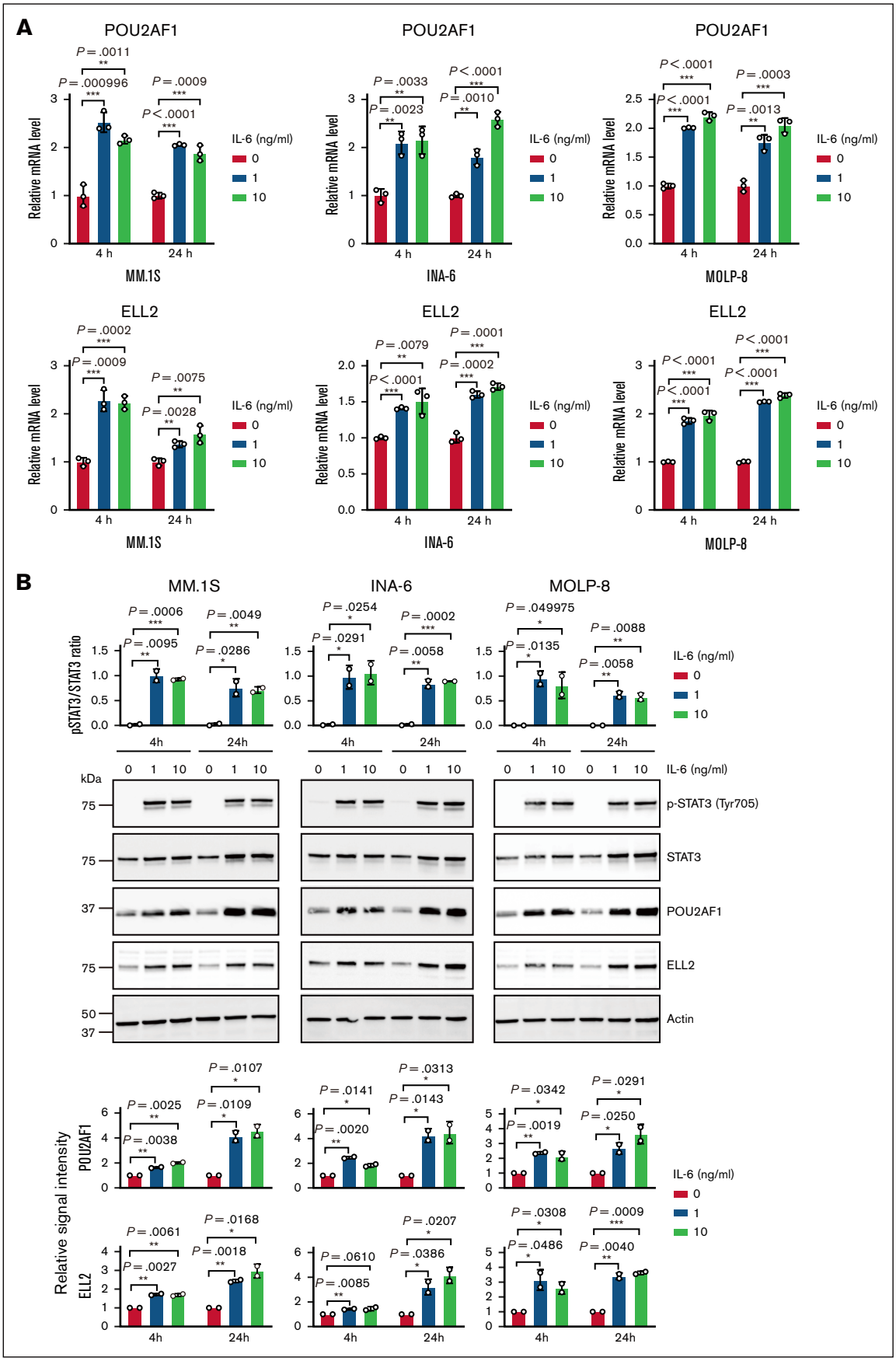

Figure 2. Validation of IL-6/JAK/STAT3 mediated POU2AF1 and ELL2 induction in MM. (A) Relative mRNA expression levels of *POU2AF1* and *ELL2* were assessed by quantitative real-time polymerase chain reaction after treatment with or without IL-6 (1 or 10 ng/mL) for 4 or 24 hours in MM cell lines (MM.1S, INA-6, and MOLP-8).

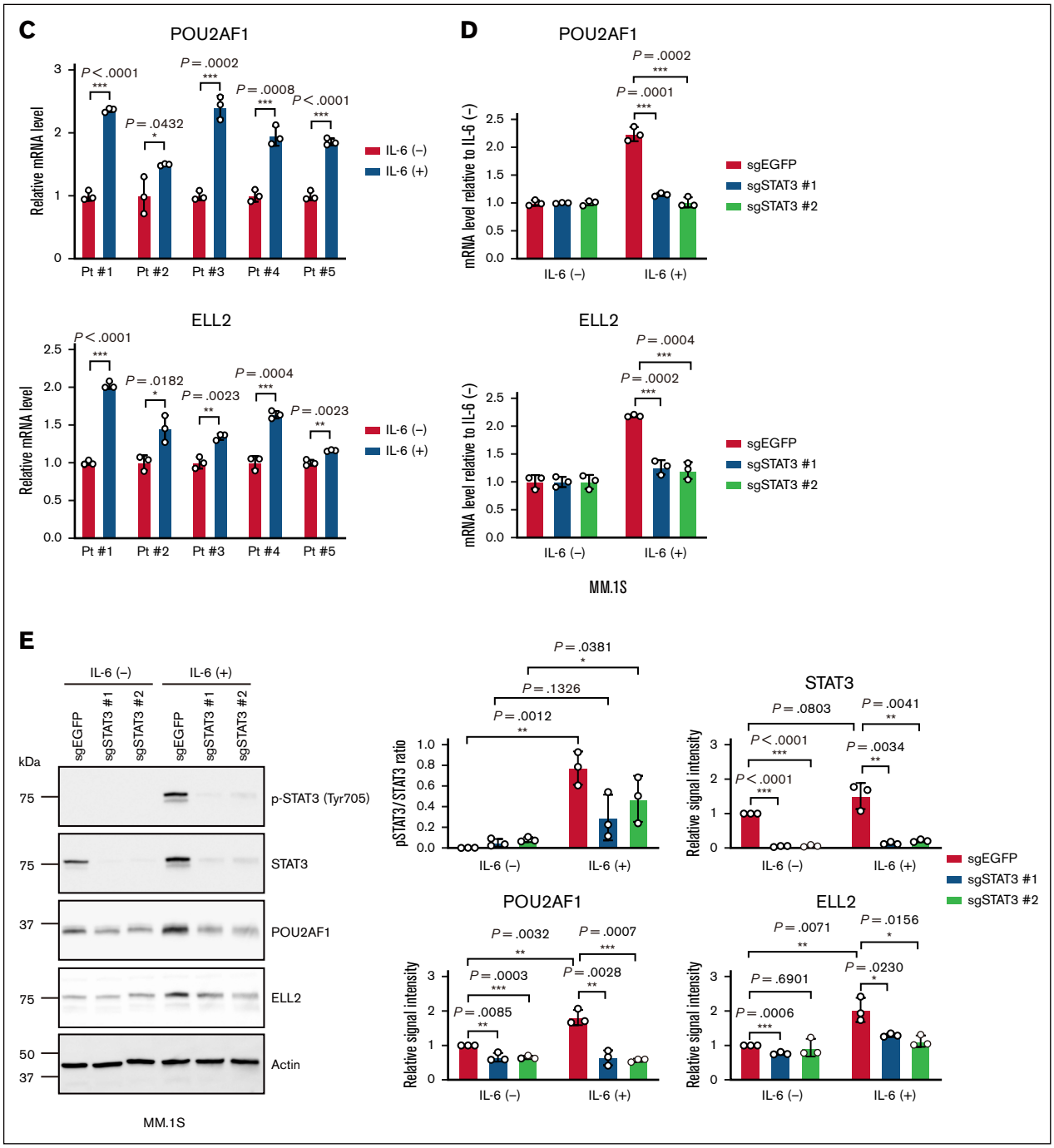

Figure 2 (continued) (B) Immunoblot analysis for p-STAT3 (Tyr705), STAT3, POU2AF1, and ELL2 in MM cell lines (MM.1S, INA-6, and MOLP-8) treated with or without IL-6 (1 or 10 ng/mL) for 4 or 24 hours. Actin served as a loading control. Shown are representative blots from 2 independent experiments. The signal intensity for each immunoblot was quantified using the ImageJ software. The pSTAT3:STAT3 ratio is shown as mean ± standard deviation (SD) (n = 2) in the top panel. POU2AF1 and ELL2 signals normalized to actin (relative to IL-6–untreated control) are shown as mean ± SD (n = 2) in the bottom panel. (C) Relative mRNA expression levels of *POU2AF1* and *ELL2* after treatment with or without IL-6 (1 ng/mL) for 4 hours in primary MM cells. (D) Relative mRNA expression levels of *POU2AF1* and *ELL2* after treatment with or without IL-6 (1 ng/mL) for 4 hours in Cas9-expressing MM.1S cells transduced with sgRNA against STAT3 (sgSTAT3) or control sgRNA against EGFP (sgEGFP). (E) Immunoblot analysis for p-STAT3 (Tyr705), STAT3, POU2AF1, and ELL2 after treatment with or without IL-6 (1 ng/ml) for 24 hours in Cas9-expressing MM.1S cells transduced with sgSTAT3 or sgEGFP. Actin served as a loading control. Shown are representative blots from 3 independent experiments. The signal intensity for each immunoblot was quantified using the ImageJ software. The pSTAT3:STAT3 ratio, along with STAT3, POU2AF1, and ELL2 signals normalized to actin (relative to IL-6–untreated sgEGFP) are shown as mean ± SD (n = 3) in the right panel. Panels A,C-D: data were normalized to expression of invariant control (*PPIA*), and the expression levels relative to IL-6–untreated control are shown as mean ± SD. Panels A-E: $^{*}P < .05$; $^{**}P < .01$; $^{***}P < .001$ (unpaired Student *t* test). Pt, patient.

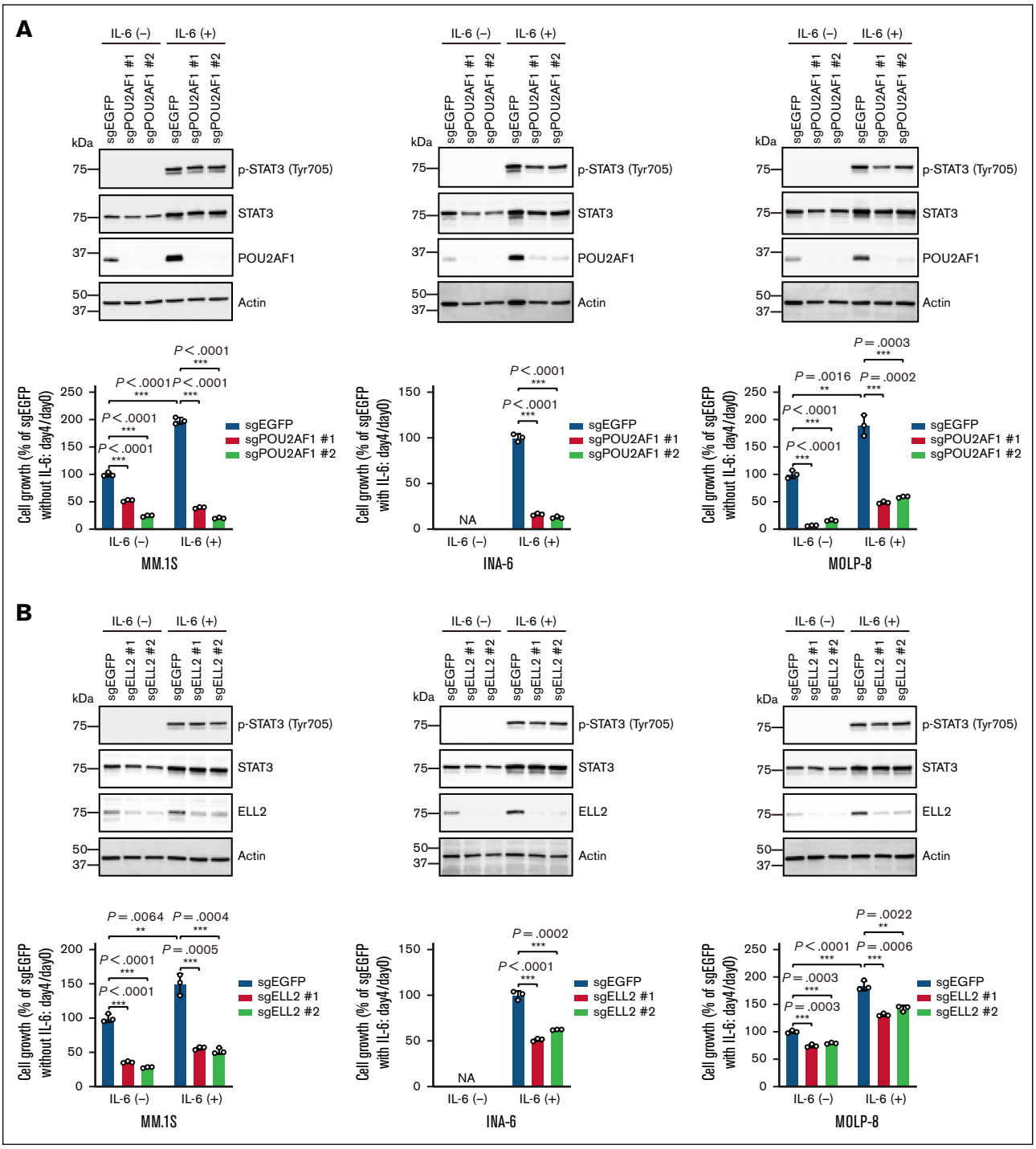

Figure 3. POU2AF1 and ELL2 are required for IL-6–mediated MM cell growth. (A-B) MM cell lines stably expressing Cas9 (MM.1S, INA-6, MOLP-8) were transduced with sgRNA targeting POU2AF1 (sgPOU2AF1), ELL2 (sgELL2), or control sgRNA targeting EGFP (sgEGFP). Three days after infection (2 days after puromycin selection) was designated as day 0. On day 0, cells were treated with or without IL-6 (1 ng/mL). On day 1, whole-cell lysates were extracted and subjected to immunoblot analysis with the indicated antibodies (top). Shown are representative blots from 2 independent experiments. On days 0 and 4, cell viability was determined by 3-(4,5-dimethylthiazol-2-yl)-2,5-diphenyl tetrasodium bromide (MTT) T assay. The cell growth rate (day 4/day 0) relative to sgEGFP without IL-6 (MM.1S and MOLP-8) or sgEGFP with IL-6 (INA-6) is shown (bottom). Data represent mean ± SD (n = 3). $^{**}P < .01$; $^{***}P < .001$ (unpaired Student *t* test). Cell growth rate could not be determined in the absence of IL-6 in INA-6 cells because almost all cells were dead within 4 days. (C) MM.1S cells stably expressing Cas9 and luciferase were transduced with sgPOU2AF1, sgELL2, or sgEGFP. One million viable cells were IV injected into NOG human IL-6 transgenic mice. The bioluminescent imaging of xenografted mice on day 43. (D) Tumor burden was serially measured by BLI. Data represent mean ± SEM. n = 3 to 4 mice per group. $P = .0199$ (sgEGFP vs sgPOU2AF1), $P = .0203$ (sgEGFP vs sgELL2) (unpaired Student *t* test). (E) Kaplan–Meier curves showing the survival of each group. $P = .0101$ (sgEGFP vs sgPOU2AF1); $P = .0101$ (sgEGFP vs sgELL2) by the log-rank test. NA, not applicable.

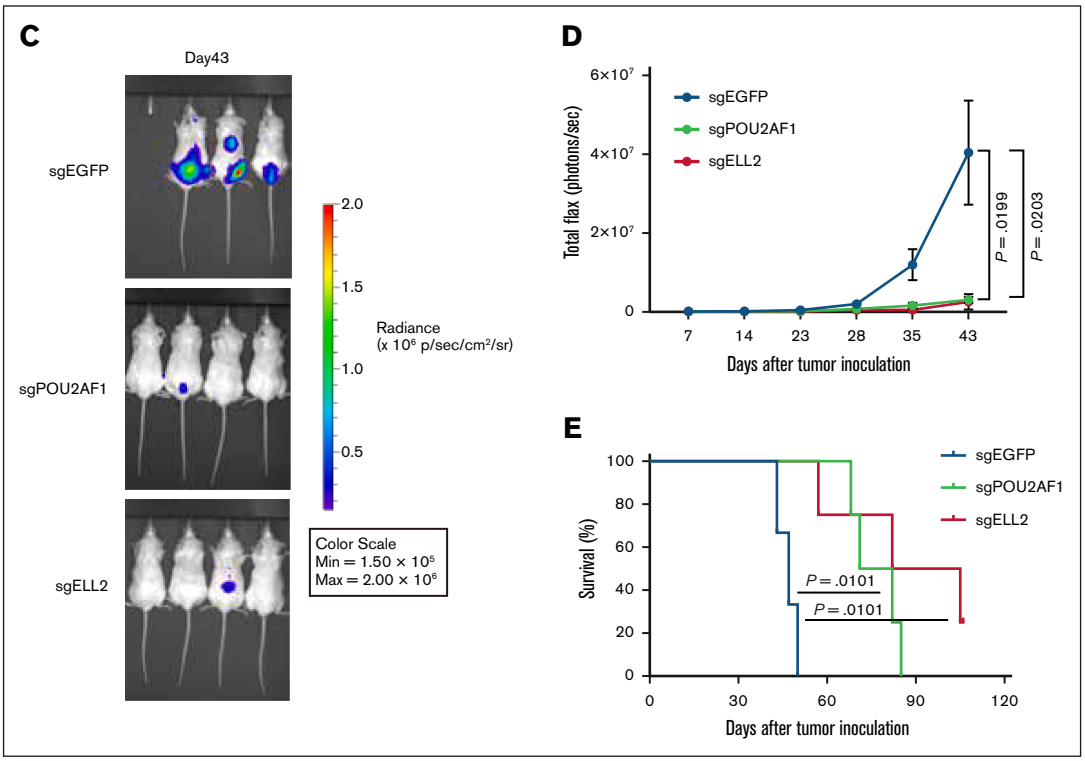

Figure 3 (continued)

the BM environment. To confirm this notion, we next used a disseminated xenograft model of MM. We IV injected *POU2AF1* and *ELL2*-depleted MM.1S cells expressing luciferase into human IL-6–expressing NOD/Shi-scid,IL-2RγKO (NOG) mice (NOG-hIL-6 Tg), and then serially monitored the tumor burden by luciferase signal. Depletion of *POU2AF1* and *ELL2* significantly delayed tumor progression (Figure 3C-D) and prolonged overall survival of the mice compared with the control group injected with sgEGFP-transduced cells (Figure 3E). These data suggest that POU2AF1 and ELL2 promote MM cell growth in the presence of IL-6 in vivo. Even though each mouse received an equal number of viable cells, it is important to consider that the observed effect could have been exaggerated, as POU2AF1 and ELL2 expression had been reduced before injecting the tumor cells.

We next sought to identify the underlying mechanisms of POU2AF1 and ELL2-mediated MM cell growth. Depletion of *POU2AF1* and *ELL2* increased apoptotic cells, as evidenced by enhanced Annexin V binding (supplemental Figure 5A-B), as well as arrested cells in S phase (supplemental Figure 5C-D) in MM.1S and INA-6 cells, although the effect of *ELL2* KO on apoptosis and cell cycle was modest in INA-6 cells (supplemental Figure 5B,D). These results indicate that POU2AF1 and ELL2 promote not only the survival of MM cells but also the proliferation of MM cells.

POU2AF1 and ELL2 positively regulate MM-specific transcriptional signatures

To decipher the molecular mechanisms underlying POU2AF1 and ELL2-induced MM cell growth and survival, we next performed differential gene expression analysis using RNA-seq. We first analyzed gene expression profiles in MM.1S cells after KO of *POU2AF1* and *ELL2* in the absence of IL-6 to understand basal functions of these factors. A total of 176 genes were downregulated, whereas 284 genes were upregulated in common between POU2AF1 and ELL2-depleted cells compared with sgEGFP-transduced cells (fold change >1.2 and false discovery rate [FDR] <0.05) (supplemental Figure 6A; supplemental Table 7). Functional enrichment analysis using the gene sets of the Molecular Signatures Database (MSigDB) hallmark showed that genes of early 2 factor (E2F) targets, G2/M checkpoint, and MYC targets were enriched in the genes downregulated by KO of *POU2AF1* and *ELL2*, whereas apoptosis-related genes were enriched among the upregulated genes (supplemental Figure 6B). These findings were in agreement with the results of apoptosis and cell cycle assays (supplemental Figure 5A-D). Enrichment analysis using the gene sets of Gene Ontology (GO) biological process also demonstrated that the expression of genes related to chromatin conformation were downregulated by KO of *POU2AF1* and *ELL2*, suggesting that these factors are associated with the maintenance of chromatin structure (supplemental Figure 6C), in line with a recent report.[30]

To further characterize the POU2AF1 and ELL2 functions, we conducted gene set enrichment analysis (GSEA). We found that the expression of signature genes related to mitochondrial functions, plasmablasts, MYC targets, tumor invasiveness, TP53-related metabolism, and translation were downregulated in POU2AF1 and ELL2-depleted MM.1S cells (Figure 4A; supplemental Table 8). Importantly, recent single-cell RNA-seq analysis using primary samples from patients with MM demonstrated that these gene signatures represent MM cell immaturity that is distinct from normal plasma cells.[47] We next investigated whether POU2AF1 and ELL2 directly regulate these MM-specific

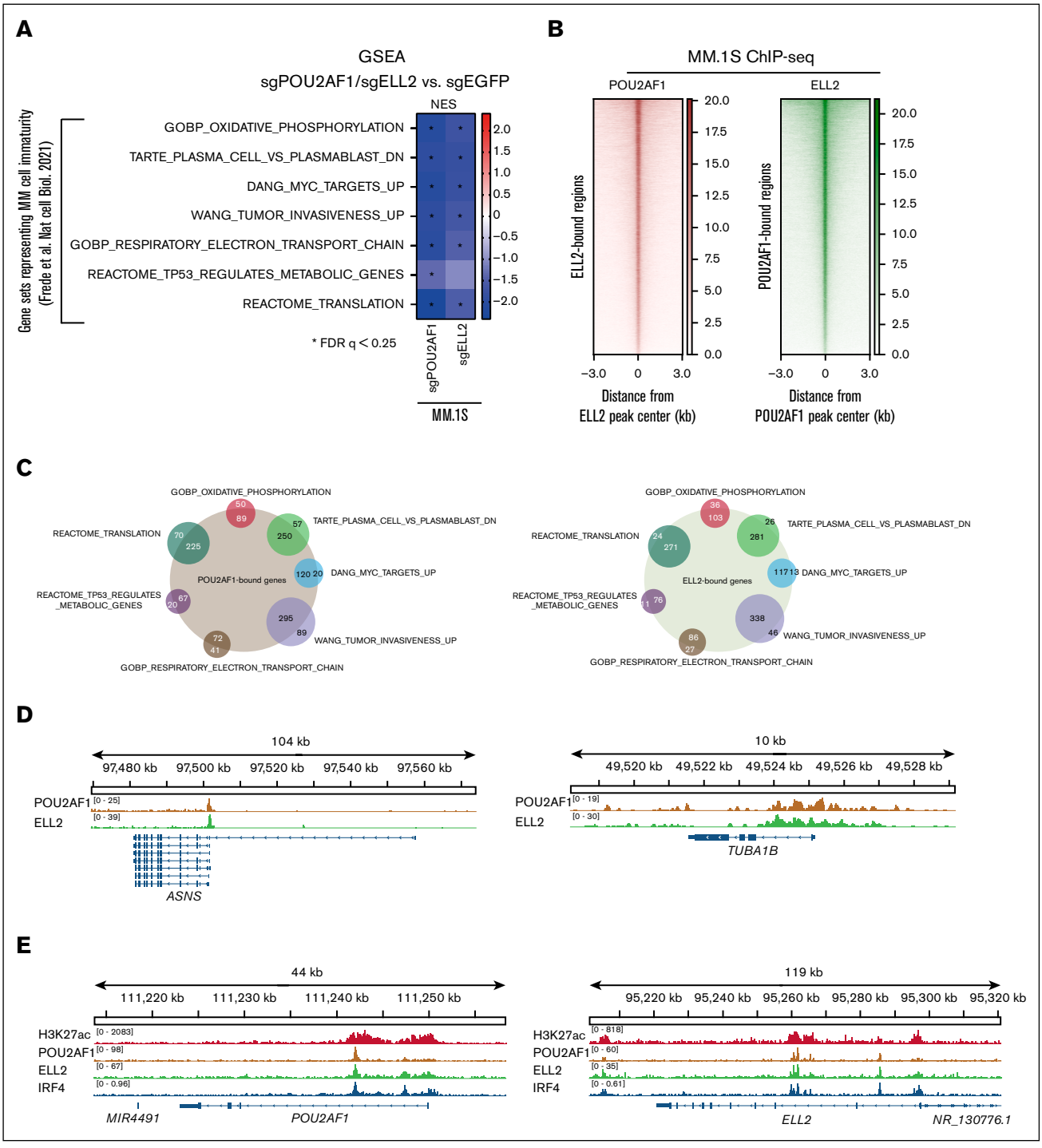

Figure 4. POU2AF1 and ELL2 positively regulate MM-distinct transcriptional signatures. (A) Heat map showing the NES from GSEA for the gene sets associated with MM cell immaturity in sgPOU2AF1- and sgELL2-transduced MM.1S cells compared with sgEGFP-transduced cells (n = 2). Asterisks indicate FDR of q <0.25. (B) Heat map displaying the distribution of POU2AF1 and ELL2 at ELL2- and POU2AF1-bound regions in MM.1S cells, determined by ChIP-seq (± 3 kb from ELL2 and POU2AF1 peak center). (C) Venn diagram illustrating the overlap of genes occupied by POU2AF1 (left) or ELL2 (right) and genes of each of the indicated gene sets. Venn diagram does not reflect the overlap of genes between each of the gene sets. (D) Gene tracks demonstrating POU2AF1 and ELL2 enrichment at the *ASNS* and *TUBA1B* gene loci (examples of the genes representing MM cell immaturity) in MM.1S cells. (E) Gene tracks showing H3K27Ac, POU2AF1, ELL2, and IRF4 signals at the *POU2AF1* and *ELL2* gene loci in MM.1S cells. The IRF4 ChIP-seq data (GSM1195560) from the Gene Expression Omnibus database was used for the analysis. (F) Heat map showing the NES from GSEA for the indicated gene sets in POU2AF1- and ELL2-high expression groups compared with POU2AF1- and ELL2-low expression groups. Newly diagnosed patients with MM (GSE2658, n = 559; GSE6401, n = 102) were divided into 2 groups on the basis of median expression level of POU2AF1 and ELL2. Asterisks indicate FDR q <0.25. (G) Heat map displaying the distribution of POU2AF1 and ELL2 at IRF4-bound regions in MM.1S cells, determined by ChIP-seq (± 3 kb from IRF4 peak center). (H) GSEA plots for the IRF4 target genes (the genes downregulated by IRF4 knockdown in MM cells) in sgPOU2AF1- and sgELL2-transduced MM.1S cells compared with sgEGFP-transduced cells. NES, normalized enrichment score.

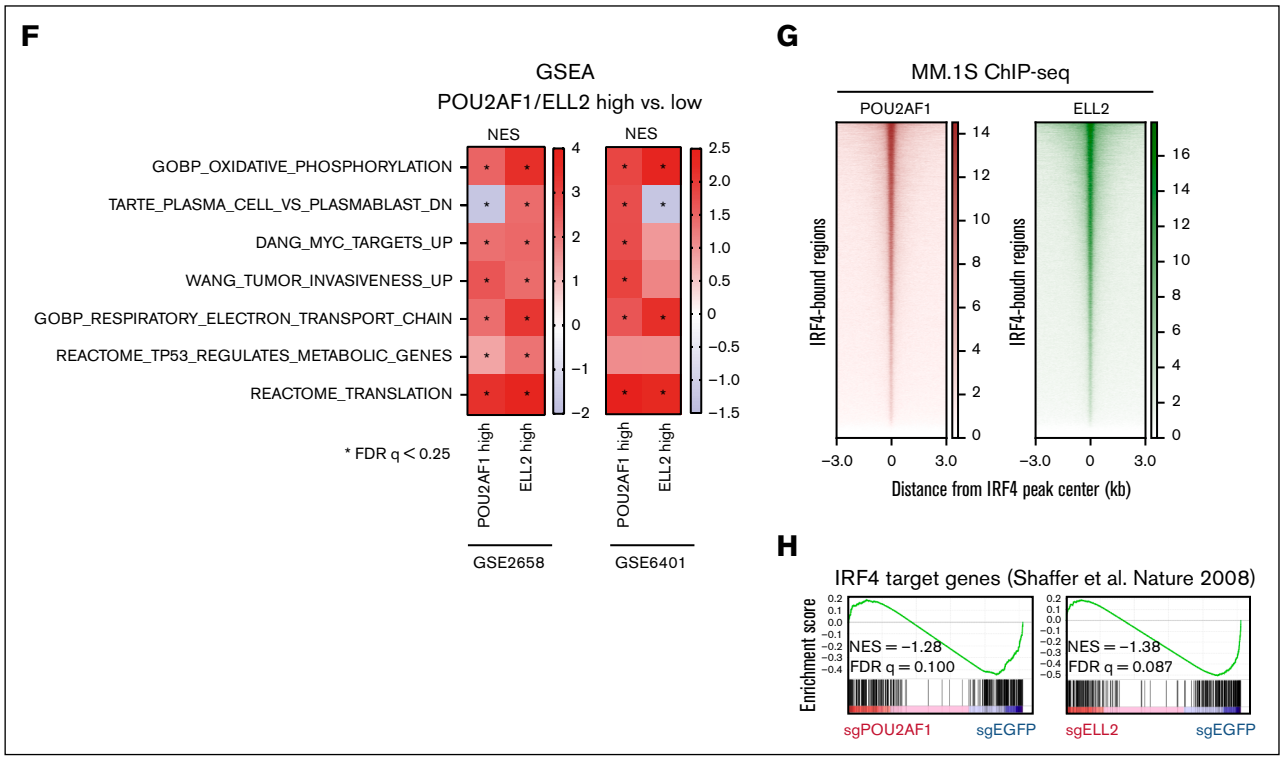

Figure 4 (continued)

transcriptional programs. Importantly, ChIP-seq analysis for POU2AF1 and ELL2 demonstrated that POU2AF1 and ELL2 coexisted with each other across genome regions (Figure 4B), and occupied most of the genes composing MM-distinct signatures (Figure 4C-D). These results suggested direct involvement of POU2AF1 and ELL2 in the regulation of MM-distinct signature genes. Since POU2AF1 and ELL2 both regulate common MM-distinct signature genes, we hypothesized that they may also control each other's expression. As expected, ChIP-seq analysis revealed that POU2AF1 binds to ELL2 regulatory elements marked by H3K27ac, and vice versa, suggesting that these factors regulate each other, creating a positive autoregulatory loop (Figure 4E). However, knocking down of either factor had minimal impact on the expression of the other (supplemental Figure 6D). These results suggest that their expression is robustly maintained by multiple regulatory mechanisms. Supporting this, ChIP-seq data showed IRF4 occupancy at the regulatory elements of both POU2AF1 and ELL2, and also showed that each of these factors bind to its own regulatory elements, suggesting an autoinduction mechanism (Figure 4E). We next analyzed gene expression profiles of samples from newly diagnosed patients with MM (GSE2658, n = 559; GSE6401, n = 102). We divided the patients into 2 groups on the basis of median expression levels of *POU2AF1* or *ELL2*. GSEA showed that most of the MM-distinct signature gene sets were upregulated in the groups of patients with higher expression of *POU2AF1* or *ELL2* compared with those with lower expression (Figure 4F; supplemental Table 8). These results support the notion that POU2AF1 and ELL2 orchestrate the MM-distinct transcriptional program characteristic of immature MM cells. We then investigated whether *POU2AF1* or *ELL2* expression correlates with clinical outcomes. No significant association was observed between these gene expressions and overall survival in patients with MM (supplemental Figure 6E).

A recent report has demonstrated that POU2AF1 interacts with IRF4 and the mammalian switch/sucrose nonfermentable chromatin remodeling (mSWI/SNF) complex, and that the formation of the POU2AF1–IRF4–mSWI/SNF complex is required for IRF4 target gene expression.[30] Consistent with this, our ChIP-seq data showed the enrichment of POU2AF1 and ELL2 signals at IRF4-bound regions (Figure 4G). Furthermore, GSEA showed that IRF4 targets in MM were significantly downregulated in both POU2AF1 and ELL2-depleted MM.1S cells (Figure 4H), further supporting the involvement of these factors in IRF4-mediated transcriptional output. Importantly, IRF4 targets in activated B lymphocytes were more profoundly downregulated than those in plasma cells in both POU2AF1 and ELL2-depleted MM.1S cells (supplemental Figure 6F), supporting the notion that POU2AF1 and ELL2 regulate transcriptional programs associated with an immature state rather than a differentiated plasma cell phenotype.

IL-6 augments MM-distinct transcriptional signatures via POU2AF1 and ELL2

Since POU2AF1 and ELL2 occupied the genes composing MM-distinct transcriptional signatures and IL-6 induced POU2AF1 and ELL2 expression in MM cells, we next ascertained whether IL-6 enhances the binding of POU2AF1 and ELL2 to the MM-distinct signature gene sets. As expected, spike-in normalized ChIP-seq for POU2AF1 and ELL2 revealed an increased binding of POU2AF1 and ELL2 to the MM-distinct signature gene sets after

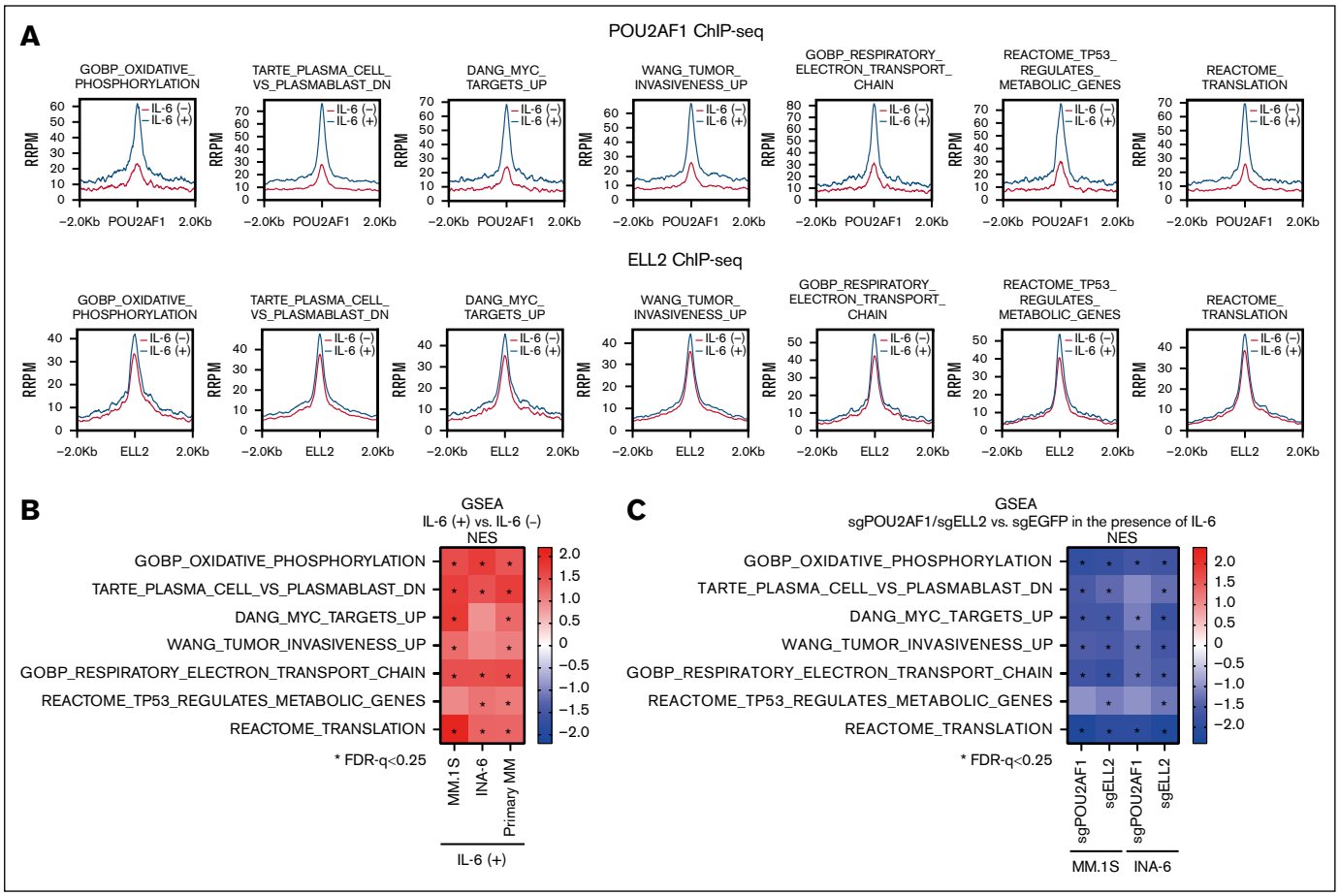

Figure 5. IL-6 induces MM-distinct transcriptional signatures via POU2AF1 and ELL2. (A) Metagene plots of POU2AF1 and ELL2 ChIP-seq signals within ± 2 kb from the center of the POU2AF1 and ELL2 binding sites of the indicated gene sets (determined in Figure 4C) in the presence or absence of IL-6 (1 ng/mL) in MM.1S cells. ChIP-seq signals were normalized to reference exogenous spiked-in *Drosophila* chromatin. RRPM, reference-normalized reads per million. (B) Heat map showing NES from GSEA for the indicated gene sets in IL-6–treated MM.1S, INA-6, and primary cells from patients with MM compared with untreated cells. Cells were treated with or without IL-6 for 24 hours. Asterisks indicate FDR q <0.25. (C) Heat map showing the NES from GSEA for the indicated gene sets in sgPOU2AF1- and sgELL2-transduced MM.1S and INA-6 cells compared to sgEGFP-transduced cells in the presence of IL-6 (1 ng/mL). Asterisks indicate FDR q <0.25. NES, normalized enrichment score.

IL-6 treatment for 24 hours, especially an increase in POU2AF1 binding was noted (Figure 5A). Consistent with the ChIP-seq results, GSEA showed that the genes of MM-distinct transcriptional signatures were upregulated after IL-6 treatment for 24 hours not only in MM cell lines (MM.1S and INA-6) but also in primary cells from patients with MM (Figure 5B; supplemental Table 8). Furthermore, the genes of MM-distinct transcriptional signatures were downregulated by depletion of *POU2AF1* and *ELL2* in the presence of IL-6 in MM.1S and INA-6 cells (Figure 5C; supplemental Table 8). Taken together, these results indicate that IL-6 augments MM-distinct transcriptional programs through POU2AF1 and ELL2 induction.

POU2AF1 mediates IL-6–induced alternative RNA splicing and facilitates nuclear speckle formation in MM cells

Transcription or epigenetic factors influence alternative RNA splicing.[48] Since past reports pointed out that MM cells exhibit distinct RNA splicing profiles,[49,50] we next examined whether POU2AF1 and ELL2 contribute to the regulation of RNA splicing. We evaluated RNA splicing profiles in MM.1S and INA-6 cells, associated with IL-6 stimulation, with or without KO of *POU2AF1* or *ELL2*. Principal component analysis of cellular RNA splicing profiles (percent spliced-in) indicated that IL-6 induced a pronounced shift in splicing status, whereas this shift was attenuated when POU2AF1 or ELL2 was depleted (Figure 6A). A comparison of individual percent spliced-in changes revealed that IL-6–driven differential splicing was partially reversed by KO of *POU2AF1* or *ELL2* (Figure 6B), and linear regression analysis confirmed inverse correlations between IL-6–induced and KO-associated RNA splicing changes in both MM cell lines, with a more significant correlation of *POU2AF1* KO- to IL-6–mediated events (Figure 6C). GO analysis of differentially spliced genes indicated that IL6-mediated splicing events were associated with cellular processes, including cell cycle and chromatin remodeling (Figure 6D).

Recent reports suggested that chromatin regulators can have a major impact on RNA splicing by maintaining homeostasis of nuclear speckles,[51,52] a membraneless nuclear compartment that controls storage and trafficking of trans-acting splicing factors.[53,54]

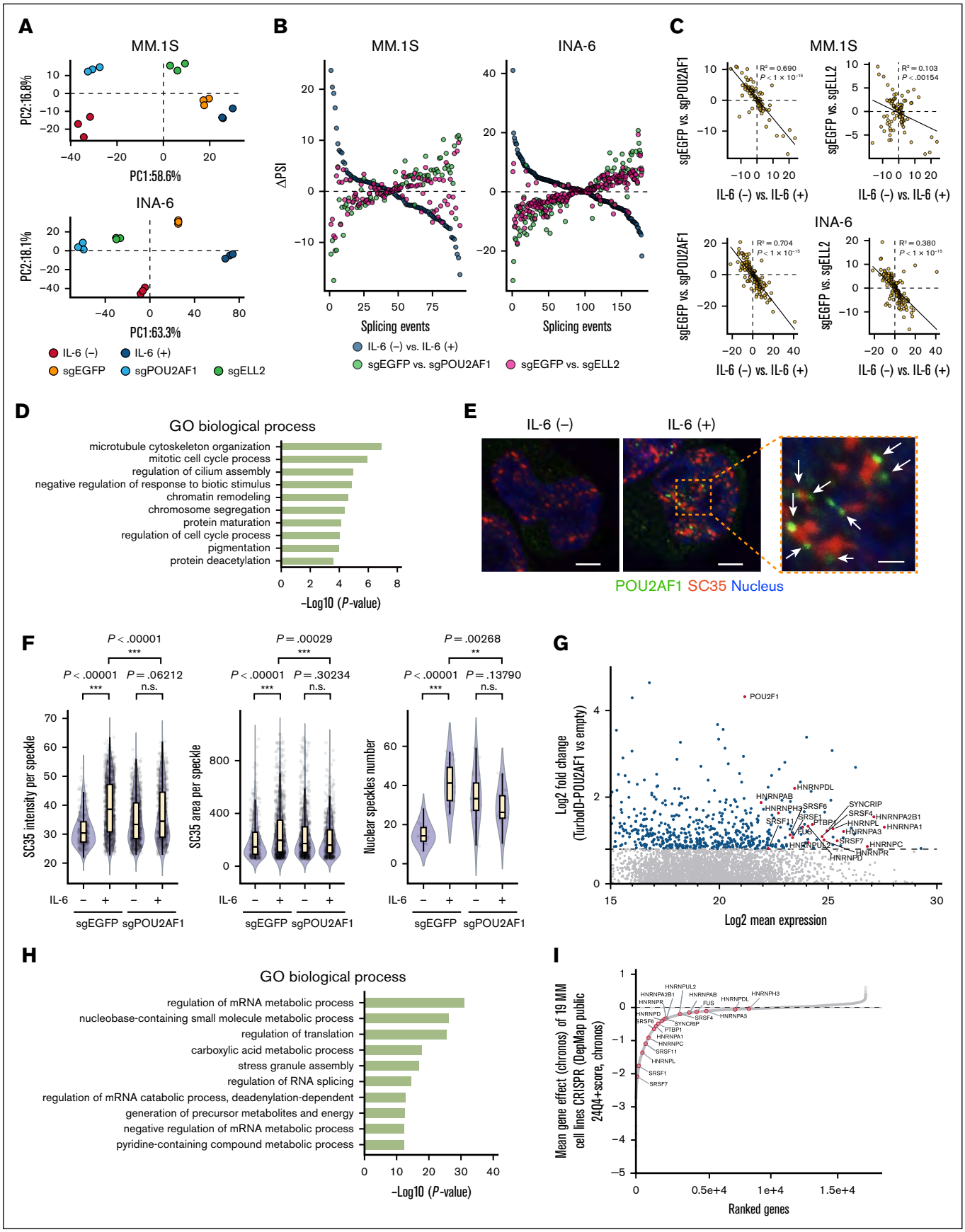

Figure 6. POU2AF1 partially mediates IL-6–induced alternative splicing in cooperation with splicing factors. (A) Principal component analysis for differentially spliced events (|Δpercent spliced-in (PSI)| ≥ 5% and FDR < 0.05) (n = 3). (B) Plot of PSI for differentially spliced events. Differential splicing events for three axis (IL-6 (-) vs IL-6 (+),

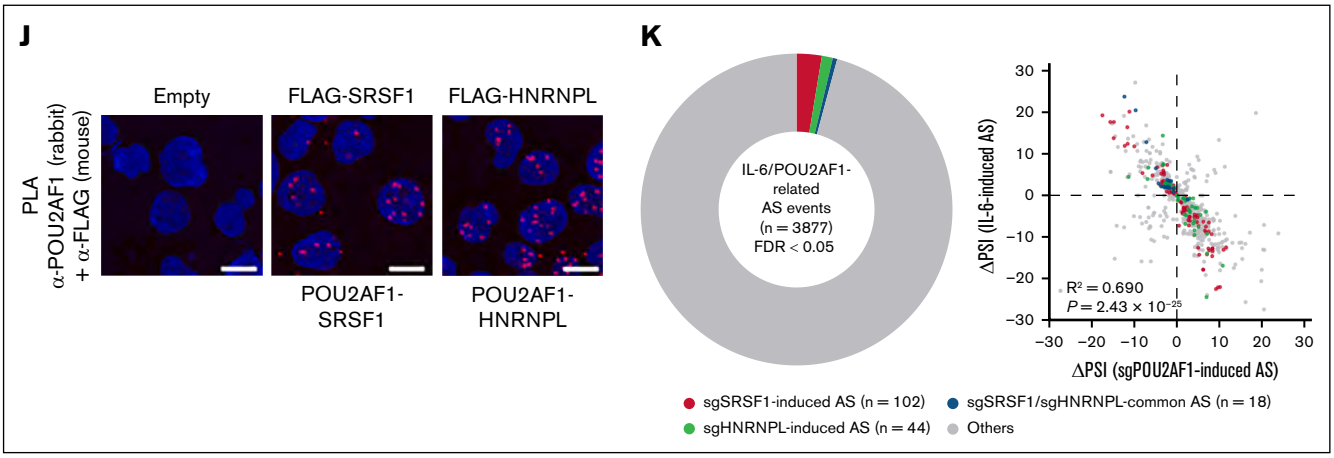

Figure 6 (continued) sgEGFP vs sgPOU2AF1, and sgEGEP vs sgELL2) are ranked by ΔPSI (IL-6 (-) vs IL-6 (+)) in MM.1S and INA-6 cells. (C) Correlation of differentially spliced events between IL-6 (-) vs IL-6 (+) and sgEGFP vs sgPOU2AF1, or between IL-6 (-) vs IL-6 (+) and sgEGEP vs sgELL2 in MM.1S and INA-6 cells. A linear regression model with $P < .05$ was considered statistically significant. Panels A-D: For KO experiments, MM.1S and INA-6 cells expressing Cas9 were transduced with sgEGFP, sgPOU2AF1, or sgELL2 in the presence of IL-6 (1 ng/mL). (D) Gene ontology (GO) analysis of differentially spliced genes (IL-6 (-) vs IL-6 (+)) ($|\Delta PSI| \geq 5\%$ and FDR < 0.05) in MM.1S and INA-6 cells. (E) Immunocytostaining of POU2AF1 and nuclear speckle marker SC35 in MM.1S cells with or without IL-6 (1 ng/mL) for 24 hours. POU2AF1, green; SC35, red; DAPI (4′,6-diamidino-2-phenylindole), blue. Scale bars, 5 μm in the overview images and 200 nm in the inset. (F) Quantification of individual nuclear speckles for fluorescent intensity (left) and area (middle) (sgEGFP/IL-6 (-), n = 318; sgEGFP/IL-6 (+), n = 902; sgPOU2AF1/IL-6 (-), n = 769; sgPOU2AF1/IL-6 (+), n = 549), as well as numbers of nuclear speckles in each cell (right) (sgEGFP/IL-6 (-), n = 22; sgEGFP/IL-6 (+), n = 23; sgPOU2AF1/IL-6 (-), n = 21; sgPOU2AF1/IL-6 (+), n = 19). Boxes, 25% (1st quartile: Q1) to 75% (3rd quartile: Q3) percentile; bars, median; upper whisker, highest data point below Q3+1.5*(Q3-Q1); lower whisker, lowest data point above Q1-1.5*(Q3-Q1); ***$P < .001$; **$P < .01$ for robust multiple comparison test. (G) MA plot showing differentially biotinylated proteins (log_2 fold change > 0.8 and log_2 mean expression > 15, TurboID-POU2AF1 vs empty [TurboID only]) in MM.1S cells (n = 2). (H) GO analysis of POU2AF1-neighboring proteins in MM.1S cells. (I) Waterfall plot showing mean CRISPR dependency score of 19 MM cell lines. Data were downloaded from DepMap portal (https://depmap.org/portal/). (J) PLA between POU2AF1 and SRSF1, or POU2AF1 and HNRNPL in MM.1S cells treated with IL-6 (1 ng/mL) for 24 hours. FLAG-tagged SRSF1 or HNRNPL were expressed in MM.1S cells, and PLA were performed using rabbit POU2AF1 antibody and mouse FLAG antibody. DAPI, blue; PLA, red. Scale bars, 10 μm. (K) Donut chart representing overlap of IL-6/POU2AF1-related and SRSF1/HNRNPL-related splicing events in MM.1S cells (left). sgSRSF1-induced alternative splicing events (AS) (n = 102), sgHNRNPL-induced AS (n = 44), and sgSRSF1/sgHNRNPL-common AS (n = 18) were observed in IL-6/POU2AF1-related AS (n = 3877). Scatterplot showing differentially spliced events analyzed in left (right panel). n.s., not significant.

Since POU2AF1 has been implicated in chromatin structure[30] and is essential for IL-6–driven RNA splicing (Figure 6A-C), we then asked whether it is associated with nuclear speckles formation. Immunocytostaining of POU2AF1 in MM.1S cells indicated that POU2AF1 localized as speckles in nucleoplasm when cells are cultured in the presence of IL-6, largely overlapping with or residing adjacent to nuclear speckles labeled by the SC35 marker (Figure 6E, white arrows in the inset), whereas POU2AF1 puncta were not visible and nuclear speckles appeared less prominent without IL-6 treatment. Quantification of nuclear speckles showed that IL-6–dependent facilitation of nuclear speckles formation was canceled when *POU2AF1* was knocked out (IL-6 (+), sgEGFP vs IL-6 (+), sgPOU2AF1 in Figure 6F), indicating that POU2AF1 is required for IL-6–dependent nuclear speckle assembly in MM cells. In addition, IL-6 treatment or *POU2AF1* KO had a minimal effect on the expression of nuclear speckle core proteins, SON and SRRM2 (supplemental Figure 7A), suggesting that the observed phenotype on nuclear speckles is not attributable to changes in core speckle protein expressions.

POU2AF1 orchestrates trans-acting splicing factors to mediate IL-6–driven RNA splicing regulation

To understand the mechanisms underlying POU2AF1-mediated splicing regulation, we examined profiling of POU2AF1-interacting proteins using proximity labeling with TurboID, which can biotinylate proximal proteins with much greater efficiency than BioID.[55] We exogenously expressed POU2AF1 fused with TurboID in MM.1S cells. After cells were lysed, biotinylated proteins were enriched using streptavidin beads and subjected to mass spectrometric analysis. We detected 559 POU2AF1-neighboring proteins (log_2 fold change > 0.8 and log_2 mean expression > 15) which included POU2F1, a known POU2AF1-interacting partner (Figure 6G; supplemental Table 9).[13-15] Intriguingly, we found that many of identified POU2AF1-interacting proteins were found to be trans-acting splicing factors (Figure 6G-H). Using DepMap CRISPR screening database that includes 19 MM cell lines, we found that MM cells were dependent on POU2AF1-neighboring splicing factors, including SRSF1 and HNRNPL (Figure 6I). SRSF1 is a crucial splicing factor that governs MM-specific alternative splicing events.[50] HNRNPL is a splicing factor indispensable for B-cell activation and survival.[56] We further confirmed that depletion of SRSF1 or HNRNPL impaired MM cell growth even in the presence of IL-6 (supplemental Figure 7B). To further validate physical interaction between POU2AF1 and SRSF1/HNRNPL, we performed a proximity ligation assay (PLA) that enables the in situ detection of protein–protein interactions within cells. Because of the limited availability of specific antibodies for these proteins, we decided to ectopically express FLAG-tagged SRSF1 or HNRNPL in MM.1S cells and conducted a PLA using a rabbit POU2AF1 antibody and a

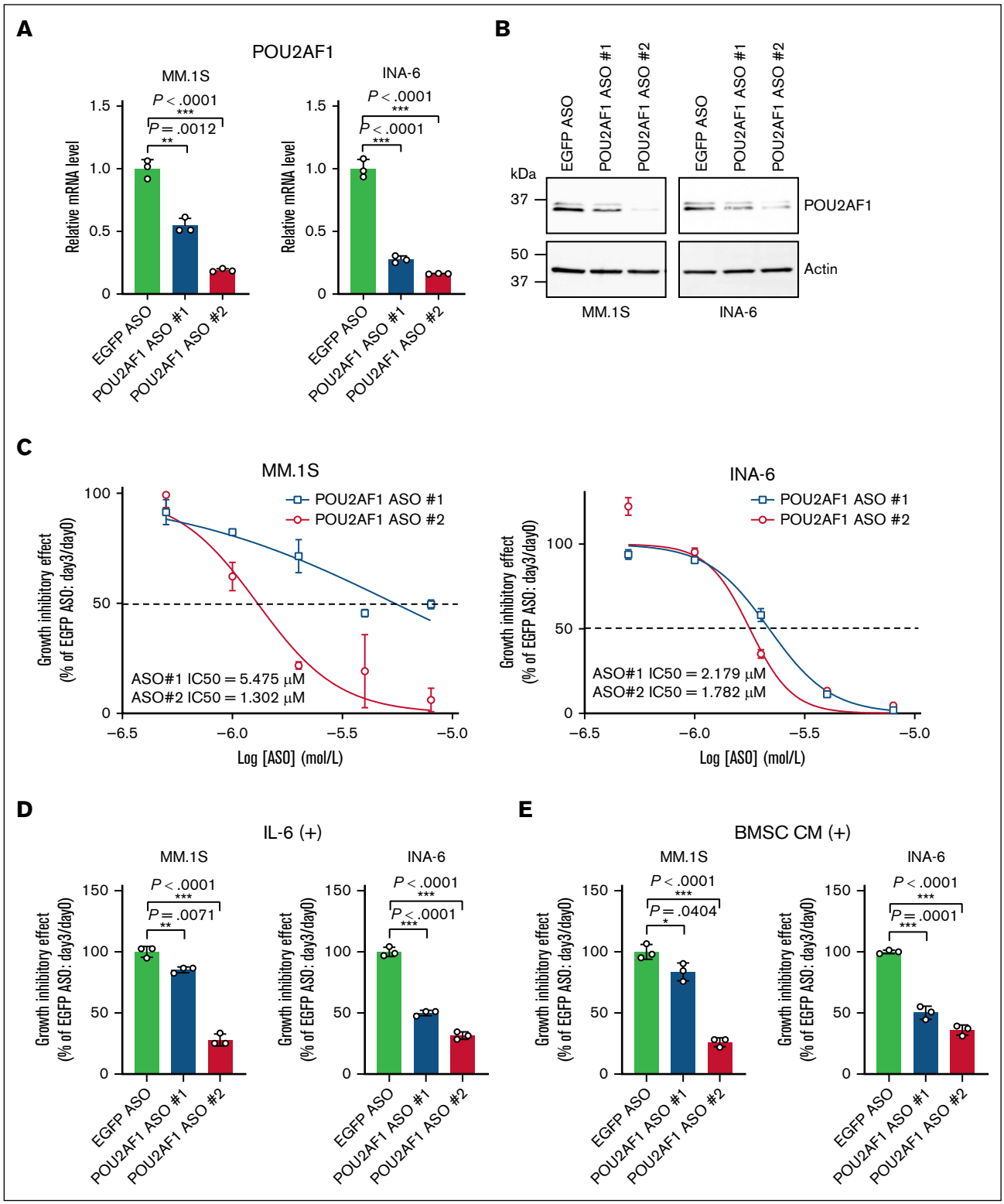

Figure 7. Gapmer ASOs targeting POU2AF1 inhibit MM cell growth. (A-E) ASOs were introduced into MM.1S and INA-6 cells by electroporation at 2 μM (A-B,D-E) or at the indicated concentrations (C). One day after electroporation was designated as day 0. (A) On day 0, total RNA was extracted and relative mRNA expression level of *POU2AF1* were assessed by quantitative real-time polymerase chain reaction. Data were normalized to expression of invariant control (*PPIA*), and the expression level relative to EGFP ASO-treated control are shown as mean ± SD (n = 3). $^{**}P < .01$; $^{***}P < .001$ (unpaired Student *t* test). (B) On day 0, whole-cell lysates were extracted and subjected to immunoblot analysis with anti-POU2AF1 antibody. Actin served as a loading control. (C-E) On day 0, cells were seeded in 96-well plates and treated with either no additives (MM.1S in panel C), IL-6 (1 ng/mL) (INA-6 in panel C; MM.1S and INA-6 in panel D), or conditioned medium from BMSCs derived from patients with MM (E). Cell viability was determined on days 0 and 3 by MTT assay, and the growth inhibitory effect (day 3/day 0) relative to EGFP ASO is shown. Data represent mean ± SD (n = 3). $^{*}P < .05$; $^{**}P < .01$; $^{***}P < .001$ (unpaired Student *t* test).

mouse FLAG antibody. Robust PLA signals were detected in the nucleus of cells expressing FLAG-tagged SRSF1 or HNRNPL, whereas a limited signal was observed in control cells (Figure 6J). We subsequently evaluated RNA splicing targets in MM cells with *SRSF1* KO or *HNRNPL* KO, and found that they accounted for 4.2% of IL-6–dependent and POU2AF1–dependent splicing events (Figure 6K; supplemental Figure 7C), suggesting that additional splicing factors are involved in POU2AF1-related RNA splicing regulation, consistent with the TurboID-based proteomics outcome.

ASO-mediated POU2AF1 inhibition suppresses MM cell growth

To extend our findings beyond genetic KO approaches, we finally examined targeting POU2AF1 using antisense oligonucleotides (ASOs). Considering therapeutic index, we selected POU2AF1 as the primary target because of its predominant expression in lymphoid cells, whereas ELL2 is ubiquitously expressed. We designed gapmer ASOs consisting of a central DNA-based internal gap and 2′-O-methoxy-ethyl–modified flanking regions that enhance the binding affinity to target mRNAs and facilitate RNase H–mediated degradation.[57] To validate ASO-mediated degradation of POU2AF1 transcripts, each ASO was cotransfected with a MYC-tagged POU2AF1 expression plasmid into HEK293T cells. We observed significant reduction of mRNA and protein levels of POU2AF1, confirming the functionality of the gapmer ASOs (supplemental Figure 8A). We next sought to deliver ASOs into MM cells. To do so, we tested and optimized electroporation method by using EGFP expression plasmid and obtained the conditions that achieved 70% to 85% transfection efficacy (supplemental Figure 8B). We then transduced ASOs into MM.1S and INA-6 cells and confirmed that expression levels of POU2AF1 were significantly inhibited, especially by POU2AF1 ASO #2 (Figure 7A-B). Consistent with this, ASOs suppressed the growth of MM.1S and INA-6 cells in a dose-dependent manner (Figure 7C). This growth inhibition was observed even in the presence of IL-6 or conditioned medium from BMSCs derived from patients (Figure 7D-E).

Discussion

Cancer cells rely on proliferation and survival mechanisms similar to those used by their lineage precursor cells. This notion called lineage dependency, has been recognized in various cancers, and lineage-survival oncogenes, with expression typically restricted to certain cell types, and are promising therapeutic targets.[58] In MM, IRF4 is a key lineage-survival oncogene required for both B-cell differentiation into plasma cells and MM cell survival.[59-61] In this study, we identify POU2AF1 and ELL2 as additional lineage-survival oncogenes in MM. POU2AF1 and ELL2 are transcription cofactors essential for B-cell development.[16,37] Although POU2AF1 expression is reduced after GC exit, we show that expression of POU2AF1 and ELL2 are epigenetically sustained through the IL-6/JAK/STAT3 pathway, which is indispensable for MM cell survival. Further, we identified POU2AF1 as a crucial factor to regulate nuclear speckles formation, ensuring the structural environment required for MM-specific RNA splicing. These findings highlight POU2AF1's key role as a lineage-survival oncogene in MM, supporting the results of previous screening studies.[30,45,46]

Single-cell RNA-seq of primary MM samples have revealed a MM-distinct transcriptional program.[47,62] This program features molecular signatures linked to mitochondrial functions, plasmablasts, MYC targets, tumor invasiveness, TP53-related metabolism, and translation, conferring a more immature profile to MM cells than normal plasma cells.[47] However, the mechanism behind this program remained unknown. Here, we show that POU2AF1 and ELL2 directly bind to MM signature loci and regulate their transcription, explaining this distinct MM state.

Our current findings indicate that POU2AF1 regulates nuclear speckles formation in an IL-6 stimulation-dependent manner, and its proximal interaction with trans-acting splicing factors are visible at specific chromatin loci in the PLA analysis. These results suggest that chromatin-bound POU2AF1 may facilitate the redistribution of splicing factors to target genes by bridging chromatin to nuclear speckles, which serve as reservoirs for splicing regulators.[53,54] Given the minimal overlap observed between IL-6/POU2AF1–regulated splicing events and those associated with SRSF1/HNRNPL, it is likely that additional splicing factors play roles in POU2AF1-mediated splicing regulation. Notably, our TurboID-based proteomic analysis identified several POU2AF1-associated splicing factors essential for MM cell survival, including SRSF7 and SRSF11. In addition, ELL2 may also contribute to RNA splicing regulation as a MM cell splicing regulator; however, the specific role of ELL2 remains to be investigated.[36,38] These observations together suggest that POU1AF1 and ELL2 may contribute to establish the characteristic RNA splicing profiles of MM.[50,63]

Targeting lineage-survival transcription factors is an effective cancer therapy, as exemplified by hormone receptor-targeted treatments for prostate and breast cancers.[58] These approaches block nuclear receptors like AR and ESR1 by inhibiting ligand-receptor complex formation. However, most transcription factors and cofactors are difficult to target with drugs.[64] Recent studies suggest that ASOs could address this challenge.[57] In this study, we demonstrate the potential of 2′-O-methoxy-ethyl–modified gapmer-type ASOs. Importantly, ASOs against POU2AF1 successfully reduce the growth of MM cells. This finding provides the rationale for seeking antisense therapies targeting lineage-survival factors, although further in vivo preclinical validation and comprehensive evaluation of therapeutic index will be required.

In conclusion, we revealed the associations of lineage-survival oncogenes with MM-distinct transcriptional program. IL-6 epigenetically induces B-cell lineage factors POU2AF1 and ELL2, which control MM-specific regulons, driving MM cell growth and survival. Our findings suggest that targeting B-cell lineage factors may represent novel therapeutic opportunities for this incurable tumor.

Acknowledgments

The authors thank Shinsuke Iida for providing INA-6 cell line.

This work was supported by grants from the Japan Society for the Promotion of Science KAKENHI (23K07862 [H.O.], 24K02482 [H.O. and G.S.], and 23K17431 [A.Y.]), the Takeda Science Foundation (A.Y. and H.O.), the Tokyo Biochemical

Research Foundation (H.O.), the Shinnihon Foundation of Advanced Medical Treatment Research (H.O.), the Princess Takamatsu Cancer Research Fund (18–25002) (H.O.), the Japanese Society of Hematology (A.Y. and H.O.), the Foundation for Promotion of Cancer Research (H.O.), the program of the Joint Usage/Research Center for Developmental Medicine, Institute of Molecular Embryology and Genetics, Kumamoto University (H.O.), and the Japan Agency for Medical Research and Development (AMED) (25ak0101263 and 25ak0101275 [A.Y.]). This research was also partially supported by Research Support Project for Life Science and Drug Discovery (Basis for Supporting Innovative Drug Discovery and Life Science Research) from AMED (grant number JP23ama121018 [S. Ohtsuki]).

Authorship

Contribution: Y.O. designed and performed the experiments, and analyzed the data; M.A. and A.Y. performed RNA splicing analysis, designed antisense oligonucleotide, and edited the manuscript; D.O. designed the experiments and analyzed the data; T. Masuda and S. Ohtsuki performed proteomic analysis; Y.K. and J.-i.Y. provided clinical samples; S.U. performed bioinformatic analysis; T.K. helped with electroporation; T.H. and G.S. helped with proximity ligation assay; S.H., S.T., S. Okada, M.N., and T. Minami analyzed the data and critically read the manuscript; and H.O. designed and performed the experiments, analyzed the data, and wrote the manuscript.

Conflict-of-interest disclosure: A.Y. received collaborative research funding from Daiichi Sankyo Co Ltd, Chugai Pharmaceutical Co Ltd, and Eisai Co Ltd, which was unrelated to the study. The remaining authors declare no competing financial interests.

ORCID profiles: Y.O., 0009-0004-1733-8515; M.A., 0000-0002-7079-4788; D.O., 0009-0006-1946-8609; T. Masuda, 0000-0003-0121-4783; Y.K., 0000-0002-8269-440X; S.U., 0000-0002-9959-3322; T.K., 0000-0001-9584-2611; S.H., 0000-0002-5748-016X; T.H., 0000-0002-3997-7471; S.T., 0000-0002-8540-7760; S. Okada, 0000-0003-3124-5206; J.-i.Y., 0000-0002-7939-2080; G.S., 0000-0003-2318-5987; S. Ohtsuki, 0000-0003-4634-7133; M.N., 0000-0002-2196-8673; T. Minami, 0000-0002-2345-1379; A.Y., 0000-0002-0664-7281; H.O., 0000-0001-8461-7398.

Correspondence: Akihide Yoshimi, Division of Cancer RNA Research, National Cancer Center Research Institute, 5-1-1 Tsukiji, Chuo-ku, Tokyo 104-0045, Japan; email: ayoshimi@ncc.go.jp; and Hiroto Ohguchi, Division of Disease Epigenetics, Institute of Resource Development and Analysis, Kumamoto University, 2-2-1 Honjo, Chuo-ku, Kumamoto 860-0811, Japan; email: ohguchi@kumamoto-u.ac.jp.

References

1. Kumar SK, Rajkumar V, Kyle RA, et al. Multiple myeloma. *Nat Rev Dis Primers*. 2017;3:17046.
2. Hirano T, Yasukawa K, Harada H, et al. Complementary DNA for a novel human interleukin (BSF-2) that induces B lymphocytes to produce immunoglobulin. *Nature*. 1986;324(6092):73-76.
3. Kawano M, Hirano T, Matsuda T, et al. Autocrine generation and requirement of BSF-2/IL-6 for human multiple myelomas. *Nature*. 1988;332(6159):83-85.
4. Klein B, Zhang XG, Jourdan M, et al. Paracrine rather than autocrine regulation of myeloma-cell growth and differentiation by interleukin-6. *Blood*. 1989;73(2):517-526.
5. Suematsu S, Matsusaka T, Matsuda T, et al. Generation of plasmacytomas with the chromosomal translocation t(12;15) in interleukin 6 transgenic mice. *Proc Natl Acad Sci U S A*. 1992;89(1):232-235.
6. Kovalchuk AL, Kim JS, Park SS, et al. IL-6 transgenic mouse model for extraosseous plasmacytoma. *Proc Natl Acad Sci U S A*. 2002;99(3):1509-1514.
7. Das R, Strowig T, Verma R, et al. Microenvironment-dependent growth of preneoplastic and malignant plasma cells in humanized mice. *Nat Med*. 2016;22(11):1351-1357.
8. Arnulf B, Lecourt S, Soulier J, et al. Phenotypic and functional characterization of bone marrow mesenchymal stem cells derived from patients with multiple myeloma. *Leukemia*. 2007;21(1):158-163.
9. de Jong MME, Kellermayer Z, Papazian N, et al. The multiple myeloma microenvironment is defined by an inflammatory stromal cell landscape. *Nat Immunol*. 2021;22(6):769-780.
10. Bisht K, Walker B, Kumar SK, et al. Chromosomal 1q21 abnormalities in multiple myeloma: a review of translational, clinical research, and therapeutic strategies. *Expert Rev Hematol*. 2021;14(12):1099-1114.
11. Hideshima T, Bergsagel PL, Kuehl WM, Anderson KC. Advances in biology of multiple myeloma: clinical applications. *Blood*. 2004;104(3):607-618.
12. Brocke-Heidrich K, Kretzschmar AK, Pfeifer G, et al. Interleukin-6-dependent gene expression profiles in multiple myeloma INA-6 cells reveal a Bcl-2 family-independent survival pathway closely associated with Stat3 activation. *Blood*. 2004;103(1):242-251.
13. Gstaiger M, Knoepfel L, Georgiev O, Schaffner W, Hovens CM. A B-cell coactivator of octamer-binding transcription factors. *Nature*. 1995;373(6512):360-362.
14. Strubin M, Newell JW, Matthias P. OBF-1, a novel B cell-specific coactivator that stimulates immunoglobulin promoter activity through association with octamer-binding proteins. *Cell*. 1995;80(3):497-506.
15. Luo Y, Roeder RG. Cloning, functional characterization, and mechanism of action of the B-cell-specific transcriptional coactivator OCA-B. *Mol Cell Biol*. 1995;15(8):4115-4124.

16. Teitell MA. OCA-B regulation of B-cell development and function. *Trends Immunol*. 2003;24(10):546-553.
17. Qin XF, Reichlin A, Luo Y, Roeder RG, Nussenzweig MC. OCA-B integrates B cell antigen receptor-CD40L- and IL 4-mediated signals for the germinal center pathway of B cell development. *EMBO J*. 1998;17(17):5066-5075.
18. Greiner A, Muller KB, Hess J, Pfeffer K, Muller-Hermelink HK, Wirth T. Up-regulation of BOB.1/OBF.1 expression in normal germinal center B cells and germinal center-derived lymphomas. *Am J Pathol*. 2000;156(2):501-507.
19. Schubart DB, Rolink A, Kosco-Vilbois MH, Botteri F, Matthias P. B-cell-specific coactivator OBF-1/OCA-B/Bob1 required for immune response and germinal centre formation. *Nature*. 1996;383(6600):538-542.
20. Kim U, Qin XF, Gong S, et al. The B-cell-specific transcription coactivator OCA-B/OBF-1/Bob-1 is essential for normal production of immunoglobulin isotypes. *Nature*. 1996;383(6600):542-547.
21. Nielsen PJ, Georgiev O, Lorenz B, Schaffner W. B lymphocytes are impaired in mice lacking the transcriptional co-activator Bob1/OCA-B/OBF1. *Eur J Immunol*. 1996;26(12):3214-3218.
22. Casellas R, Jankovic M, Meyer G, et al. OcaB is required for normal transcription and V(D)J recombination of a subset of immunoglobulin kappa genes. *Cell*. 2002;110(5):575-585.
23. Heckman CA, Duan H, Garcia PB, Boxer LM. Oct transcription factors mediate t(14;18) lymphoma cell survival by directly regulating bcl-2 expression. *Oncogene*. 2006;25(6):888-898.
24. Chapuy B, McKeown MR, Lin CY, et al. Discovery and characterization of super-enhancer-associated dependencies in diffuse large B cell lymphoma. *Cancer Cell*. 2013;24(6):777-790.
25. Wang T, Birsoy K, Hughes NW, et al. Identification and characterization of essential genes in the human genome. *Science*. 2015;350(6264):1096-1101.
26. Song S, Cao C, Choukrallah MA, et al. OBF1 and Oct factors control the germinal center transcriptional program. *Blood*. 2021;137(21):2920-2934.
27. Zhao C, Inoue J, Imoto I, et al. POU2AF1, an amplification target at 11q23, promotes growth of multiple myeloma cells by directly regulating expression of a B-cell maturation factor, TNFRSF17. *Oncogene*. 2008;27(1):63-75.
28. Toman I, Loree J, Klimowicz AC, et al. Expression and prognostic significance of Oct2 and Bob1 in multiple myeloma: implications for targeted therapeutics. *Leuk Lymphoma*. 2011;52(4):659-667.
29. Jahn L, Hombrink P, Hagedoorn RS, et al. TCR-based therapy for multiple myeloma and other B-cell malignancies targeting intracellular transcription factor BOB1. *Blood*. 2017;129(10):1284-1295.
30. He T, Xiao L, Qiao Y, et al. Targeting the mSWI/SNF complex in POU2F-POU2AF transcription factor-driven malignancies. *Cancer Cell*. 2024;42(8):1336-1351.e9.
31. Shilatifard A, Duan DR, Haque D, et al. ELL2, a new member of an ELL family of RNA polymerase II elongation factors. *Proc Natl Acad Sci U S A*. 1997;94(8):3639-3643.
32. Lin C, Smith ER, Takahashi H, et al. AFF4, a component of the ELL/P-TEFb elongation complex and a shared subunit of MLL chimeras, can link transcription elongation to leukemia. *Mol Cell*. 2010;37(3):429-437.
33. Luo Z, Lin C, Shilatifard A. The super elongation complex (SEC) family in transcriptional control. *Nat Rev Mol Cell Biol*. 2012;13(9):543-547.
34. Shell SA, Martincic K, Tran J, Milcarek C. Increased phosphorylation of the carboxyl-terminal domain of RNA polymerase II and loading of polyadenylation and cotranscriptional factors contribute to regulation of the ig heavy chain mRNA in plasma cells. *J Immunol*. 2007;179(11):7663-7673.
35. Martincic K, Alkan SA, Cheatle A, Borghesi L, Milcarek C. Transcription elongation factor ELL2 directs immunoglobulin secretion in plasma cells by stimulating altered RNA processing. *Nat Immunol*. 2009;10(10):1102-1109.
36. Benson MJ, Aijo T, Chang X, et al. Heterogeneous nuclear ribonucleoprotein L-like (hnRNPLL) and elongation factor, RNA polymerase II, 2 (ELL2) are regulators of mRNA processing in plasma cells. *Proc Natl Acad Sci U S A*. 2012;109(40):16252-16257.
37. Park KS, Bayles I, Szlachta-McGinn A, et al. Transcription elongation factor ELL2 drives Ig secretory-specific mRNA production and the unfolded protein response. *J Immunol*. 2014;193(9):4663-4674.
38. Nelson AM, Carew NT, Smith SM, Milcarek C. RNA splicing in the transition from B cells to antibody-secreting cells: the influences of ELL2, small nuclear RNA, and endoplasmic reticulum stress. *J Immunol*. 2018;201(10):3073-3083.
39. Swaminathan B, Thorleifsson G, Joud M, et al. Variants in ELL2 influencing immunoglobulin levels associate with multiple myeloma. *Nat Commun*. 2015;6:7213.
40. Li N, Johnson DC, Weinhold N, et al. Genetic predisposition to multiple myeloma at 5q15 is mediated by an ELL2 enhancer polymorphism. *Cell Rep*. 2017;20(11):2556-2564.
41. Ali M, Ajore R, Wihlborg AK, et al. The multiple myeloma risk allele at 5q15 lowers ELL2 expression and increases ribosomal gene expression. *Nat Commun*. 2018;9(1):1649.
42. Du Z, Weinhold N, Song GC, et al. A meta-analysis of genome-wide association studies of multiple myeloma among men and women of African ancestry. *Blood Adv*. 2020;4(1):181-190.
43. Ajore R, Niroula A, Pertesi M, et al. Functional dissection of inherited non-coding variation influencing multiple myeloma risk. *Nat Commun*. 2022;13(1):151.

44. Barretina J, Caponigro G, Stransky N, et al. The Cancer Cell Line Encyclopedia enables predictive modelling of anticancer drug sensitivity. *Nature*. 2012;483(7391):603-607.
45. Ghandi M, Huang FW, Jane-Valbuena J, et al. Next-generation characterization of the Cancer Cell Line Encyclopedia. *Nature*. 2019;569(7757):503-508.
46. de Matos Simoes R, Shirasaki R, Downey-Kopyscinski SL, et al. Genome-scale functional genomics identify genes preferentially essential for multiple myeloma cells compared to other neoplasias. *Nat Cancer*. 2023;4(5):754-773.
47. Frede J, Anand P, Sotudeh N, et al. Dynamic transcriptional reprogramming leads to immunotherapeutic vulnerabilities in myeloma. *Nat Cell Biol*. 2021;23(11):1199-1211.
48. Boumpas P, Merabet S, Carnesecchi J. Integrating transcription and splicing into cell fate: transcription factors on the block. *Wiley Interdiscip Rev RNA*. 2023;14(2):e1752.
49. Bauer MA, Ashby C, Wardell C, et al. Differential RNA splicing as a potentially important driver mechanism in multiple myeloma. *Haematologica*. 2021;106(3):736-745.
50. Aktas Samur A, Fulciniti M, Avet-Loiseau H, et al. In-depth analysis of alternative splicing landscape in multiple myeloma and potential role of dysregulated splicing factors. *Blood Cancer J*. 2022;12(12):171.
51. Rivera C, Verbel-Vergara D, Arancibia D, et al. Revealing RCOR2 as a regulatory component of nuclear speckles. *Epigenetics Chromatin*. 2021;14(1):51.
52. Yu R, Roseman S, Siegenfeld AP, et al. CTCF/RAD21 organize the ground state of chromatin-nuclear speckle association. *Nat Struct Mol Biol*. 2025;32(6):1069-1080.
53. Spector DL, Lamond AI. Nuclear speckles. *Cold Spring Harb Perspect Biol*. 2011;3(2):a000646.
54. Bhat P, Chow A, Emert B, et al. Genome organization around nuclear speckles drives mRNA splicing efficiency. *Nature*. 2024;629(8014):1165-1173.
55. Branon TC, Bosch JA, Sanchez AD, et al. Efficient proximity labeling in living cells and organisms with TurboID. *Nat Biotechnol*. 2018;36(9):880-887.
56. Subramani PG, Fraszczak J, Helness A, Estall JL, Moroy T, Di Noia JM. Conserved role of hnRNPL in alternative splicing of epigenetic modifiers enables B cell activation. *EMBO Rep*. 2024;25(6):2662-2697.
57. Roberts TC, Langer R, Wood MJA. Advances in oligonucleotide drug delivery. *Nat Rev Drug Discov*. 2020;19(10):673-694.
58. Garraway LA, Sellers WR. Lineage dependency and lineage-survival oncogenes in human cancer. *Nat Rev Cancer*. 2006;6(8):593-602.
59. Iida S, Rao PH, Butler M, et al. Deregulation of MUM1/IRF4 by chromosomal translocation in multiple myeloma. *Nat Genet*. 1997;17(2):226-230.
60. Shaffer AL, Emre NC, Lamy L, et al. IRF4 addiction in multiple myeloma. *Nature*. 2008;454(7201):226-231.
61. Amanda S, Tan TK, Iida S, Sanda T. Lineage- and stage-specific oncogenicity of IRF4. *Exp Hematol*. 2022;114:9-17.
62. Dang M, Wang R, Lee HC, et al. Single cell clonotypic and transcriptional evolution of multiple myeloma precursor disease. *Cancer Cell*. 2023;41(6):1032-1047.e4.
63. Ogiya D, Chyra Z, Verselis SJ, et al. Identification of disease-related aberrantly spliced transcripts in myeloma and strategies to target these alterations by RNA-based therapeutics. *Blood Cancer J*. 2023;13(1):23.
64. Bradner JE, Hnisz D, Young RA. Transcriptional addiction in cancer. *Cell*. 2017;168(4):629-643.